International Journal of Academic Research
ISSN: 2348-7666 Vol.1 Issue-4 (1) (Special), October-December 2014

Spectroscopic Studies of Natural Mineral: Tennantite

G.S.C. Bose[1,4], B. Venkateswara Rao[2], A.V. Chandrasekhar[3], R.V.S.S.N.Ravikumar[4]
[1]Department of Physics, J.K.C. College, Guntur-522006, A.P., India
[2]Department of Physics, S.S.N. College, Narasaraopet-522601, A.P., India
[3]Department of Physics, S.V. Arts College, Tirupati-517502, A.P., India
[4]Department of Physics, Acharya Nagarjuna University, Nagarjuna Nagar-522510, A.P., India,

Abstract
The XRD, optical, EPR and FT-IR spectral analyses of copper bearing natural mineral Tennantite of Tsumeb, Namibia are carried out. From the powder XRD pattern of sample confirms the crystal structure and average crystallite size is 34 nm. Optical absorption studies exhibited several bands and the site symmetry is tetrahedral. EPR spectra at room and liquid nitrogen temperature also reveals the site symmetry of copper ions as tetrahedral. From FT-IR spectrum is characteristic vibrational bands of As-OH, S-O, C-O and hydroxyl ions.
Keywords: Tennantite, XRD, optical, EPR, FT-IR, crystal field parameters

1 Introduction

The mineral was first described for an occurrence in Cornwall, England in 1819 and named after the English Chemist Smithson Tennant (1761-1815).Tennantite is a copper arsenic sulfosalt mineral with an ideal formula $Cu_{12}As_4S_{13}$. Due to variable substitution of copper by iron and zinc the formula is $Cu_6[Cu_4(Fe, Zn)_2]As_4S_{13}$ [1]. It is gray-black, steel-gray, iron-gray or black in colour. A closely related mineral, tetrahedrite ($Cu_{12}Sb_4S_{13}$) has antimony substituting for arsenic and the two form a solid solution series. The two have very similar properties and is often difficult to distinguish between tennantite and tetrahedrite. Iron, zinc and silver substitute up to about 15% for the copper site [2]. Copper occurs naturally in the Earth's crust in a variety of forms. Its major sulphide mineral ores include chalcopyrite $CuFeS_2$, bornite Cu_5FeS_4, chalcocite Cu_2S and covellite CuS. Copper can be found in carbonate deposits as azurite $Cu_3(CO_3)_2(OH)_2$ and malachite $Cu_2(CO_3)(OH)_2$; and in silicate deposits as chrysocolla $(Cu,Al)_2H_2Si_2O_5(OH)_4{\cdot}nH_2O$ and dioptase $CuSiO_2(OH)_2$); and as pure native copper. Copper is extracted from its ore by either smelting with refining [3] or leaching with electro-winning [4]. Copper extraction through pyrometallurgical processing of concentrates relies heavily on copper sulphides and to a lesser degree on copper oxides, which are processed hydro-metallurgically. Nowadays, many of the new copper sulphide mineral deposits found are complex in nature and often found in association with

antimony and arsenic minerals [5,6] which render the concentrate unsuitable as a feedstock for smelting due to their antimony, arsenic and mercury contents which can create serious environmental problems [7-9] and even affect the quality of the copper product [10]. The common impurity minerals found in association with copper ores include tetrahedrite ($Cu_{12}Sb_4S_{13}$), jamesonite ($Pb_4FeSb_6S_{14}$), bournonite ($PbCuSbS_3$), tennantite ($Cu_{12}As_4S_{13}$) and enargite (Cu_3AsS_4). These minerals are economically attractive; however, the content of antimony and arsenic reduces their economic values effectively [11].

Copper, in divalent oxidation state has been found to exhibit many types of coordination ranging from square planar to distorted trigonal bipyramidal, square pyramidal and octahedral co-ordinations. Superposed on these coordination polyhedra, there is a general distortion of four short and one or two longer bonds. This is the characteristic of divalent copper ion. The optical and EPR spectral studies of Cu^{2+} in octahedral sites of natural minerals have been studied in great detail [12-14]. This, however, has not been the case for Cu^{2+} in tetrahedral coordination; only a few cases have been reported [15,16]. In view of this the present spectroscopic investigations of natural mineral sample tennantite are carried out. The main purpose of the present study is to determine the valance state and site symmetry of Cu^{2+} ion and any other impurities present in the mineral.

2 Crystal Structure

Fig. 1 shows natural tennantite mineral. The crystal structures of the tetrahedrite-tennantite family can be interpreted either as an omission derivative of the sphalerite structure type, with ensuing substitution and insertion of cations and anions, or as a maximally collapsed sodalite-type tetrahedral framework (Fig.2).

Fig. 1 Tennantite natural mineral

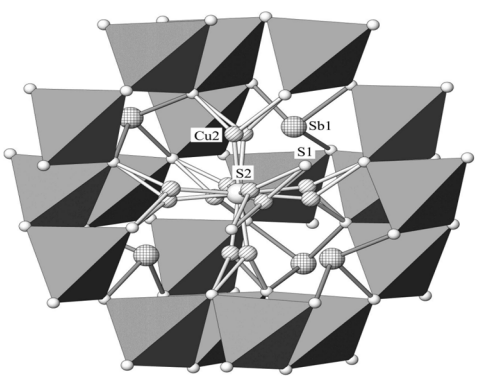

Fig. 2 Crystal structure of tennantite

Voids in the tetrahedral framework have a shape of large truncated tetrahedra, so-called 'Laves polyhedra'. The single-tetrahedral walls separating them are all what remains of the tetrahedral framework of the cubic ZnS type. These walls consist of rings of six 'Cu1'S14 tetrahedra ('Cu1' site accommodates Cu as well as all tetrahedrally coordinated divalent cations substituting for copper) around a trigonal coordination pyramid SbS_3 (or AsS_3), which stands for an original tetrahedron of the framework as well. Four such pyramids point into the void, which, besides the lone electron pairs of these metalloids, contains a 'spinner' of six triangularly coordinated Cu2 sites. These Cu sites share a single S2 atom in the centre of the cavity and each Cu2 is coordinated to two additional S1 atoms belonging to the tetrahedral framework (Fig. 2). The ring of tetrahedra mentioned above is a collapsed version of the ring of six tetrahedra around a hexagonal opening in the type sodalite structure.

3 Experimental

3.1Sample Collection

Tennantite natural mineral sample was donated by Mr. F. Ebbult, Institute of Mineralogy and Petrograph, ETH Zentrum, Switzerland and originated from Tsumeb, Namibia. Tennantite sample could not be cut into single crystals, because of non-availability of sufficient quantity of the minerals.

3.2 Characterizations

Powder XRD pattern of the collected sample was recorded on PANalytical Xpert Pro diffractometer with CuKα radiation. Fine powdered mineral samples mixed with nujol (liquid paraffin) were used for optical absorption studies. The optical spectra are recorded in the range from 400–2600 nm on JASCO V-670 spectrophotometer. The EPR spectra of the polycrystalline samples taken into EPR quartz tubes are recorded both at room and liquid nitrogen temperatures on JEOL–TE 100 ESR spectrometer operating at X-band frequency 8.985GHz. Bruker Alpha FT-IR spectrophotometer is used for recording FT-IR spectrum of tennantite mineral in the region 500-4000 cm^{-1}.

4 Results and Discussion

4.1 Power X-ray Diffraction Study

Fig. 3 shows powder XRD pattern of tennantite sample depicted against the Bragg's angle that ranged from 10^0 to 75^0. The peak positions observed in Fig. 3. are well matched with standard diffraction data of JCPDS file no. 43-1478. The diffraction data is indexed to a cubic crystal system and the corresponding lattice cell parameter is evaluated as a = 10.2201 Å.

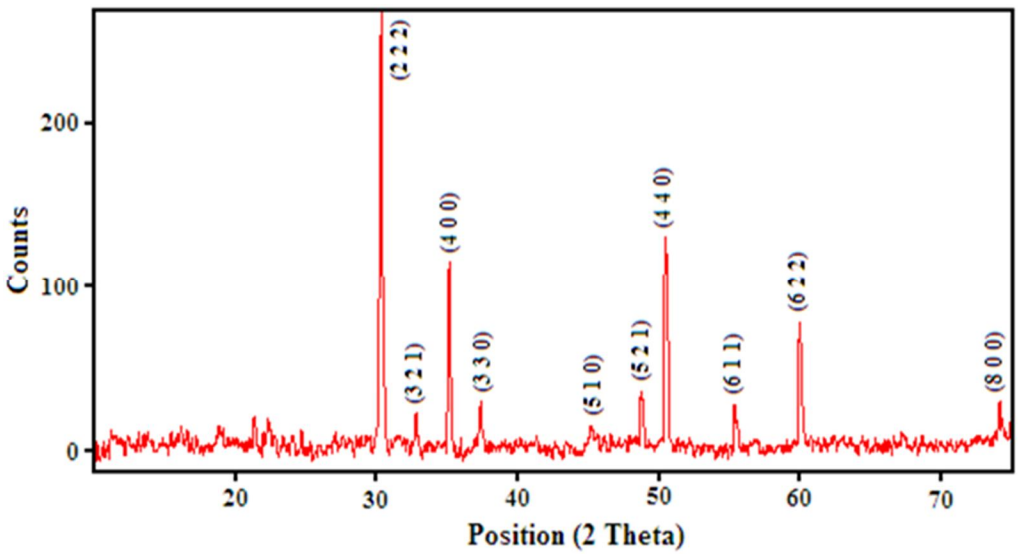

Fig. 3 Powder XRD pattern of tennantite mineral

The average crystallite size of the collected sample is calculated by using Debye-Scherrer's formula, **$D = (k\lambda/\beta\cos\theta)$,** where k is a constant (about 0.9), λ is wavelength of X-ray radiation (1.5405 Å), β is full width at half maximum (FWHM) intensity of the diffraction line and θ is diffraction angle. Based on the value of FWHM, the average crystallite size is estimated to be 34 nm, which is in the order of nanosize. Accordingly, it is possible to calculate both of the strain ε, dislocation density δ to have more information about the structural characteristics of prepared sample [17, 18]. The average strain of collected sample was calculated by Stokes-Wilson equation $\varepsilon_{str} = \beta/4\tan\theta$ and dislocation density was calculated from the relation $\delta = 15\varepsilon/aD$.

$\varepsilon_{str} = 0.283 \times 10^{-3}$ and $\delta = 0.122 \times 10^{15}$ lines/m

4.2 Optical absorption study

The optical absorption spectrum gives rich information regarding site symmetry and distortions. Optical absorption spectrum of tennantite mineral exhibit five bands in the region 350-550 nm and three discrete bands in the region 2000-2500 nm (NIR region) which are shown in Fig. 4 and Fig. 5 respectively.

The bands in the shorter wavelength region (350-550 nm) are characteristic of Fe(III) ions in tetrahedral symmetry. The relative intense bands observed at 541 nm (18484 cm^{-1}) and 473 nm (21141 cm^{-1}) are attributed to $^6A_1(S) \rightarrow {}^4T_1(G)$

and to $^6A_1(S) \rightarrow {}^4T_2(G)$ transitions respectively.

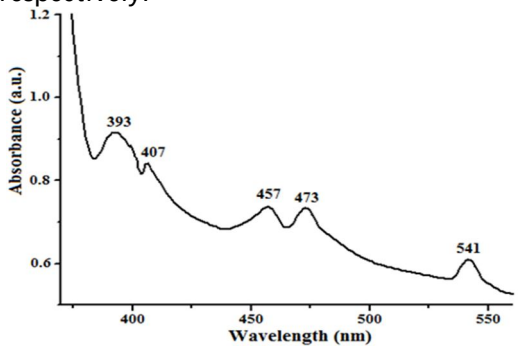

Fig. 4 Optical absorption spectrum of tennantite in the region 350-550 nm

With the help of Tanabe-Sugano diagram the other bands observed at 457 nm (21881 cm^{-1}), 407 nm (24570 cm^{-1}) and 393 nm (25445 cm^{-1}) are attributed to the transitions $^6A_1(S) \rightarrow {}^4E(G) + {}^4A_1(G)$, $^6A_1(S) \rightarrow {}^4T_2(D)$ and $^6A_1(S) \rightarrow {}^4E(D)$ respectively [19]. Table 3.1 shows the band head data and assignments of Fe^{3+} ions in tennantite mineral. By solving Tanabe-Sugano matrices with Tree's correction (α = 90), the following crystal field (Dq) and Racah (B, C) parameters are evaluated:

Dq = 450, B = 685 and C = 2650 cm^{-1}

As shown in Fig. 5, the bands in NIR region (2000-2500 nm) are attributed to Cu(II) ions in tetrahedral environment. The optical absorption spectrum of tennantite mineral reveal three bands at 2202, 2309 and 2349 nm (NIR region) which are attributed to the transitions $^2B_2 \rightarrow {}^2A_1$, $^2B_2 \rightarrow {}^2B_1$ and $^2B_2 \rightarrow {}^2E$ respectively. From these assignments the crystal field (Dq) and tetragonal field (Ds, Dt) parameters are evaluated using the following expressions.

$^2B_2 \rightarrow {}^2A_1$: 10Dq – 4Ds – 5Dt

$^2B_2 \rightarrow {}^2B_1$: 10Dq

$^2B_2 \rightarrow {}^2E$: -3Ds + 5D

The crystal field (Dq) and tetragonal field (Ds, Dt) parameters are evaluated as
Dq = 433, Ds = -638 and Dt = 468 cm^{-1}.

Table 1 Band head data and assignments of Fe^{3+} ions in tennantite mineral

Transition From $^6A_1 \rightarrow$	Band position Wavelength nm	Wavenumber (cm^{-1}) observed	calculated
$^4E(D)$	393	25445	25469
$^4T_2(D)$	407	24570	24570
$^4A_1(G) + {}^4E(G)$	457	21881	21883
$^4T_2(G)$	473	21141	21106
$^4T_1(G)$	541	18484	18455

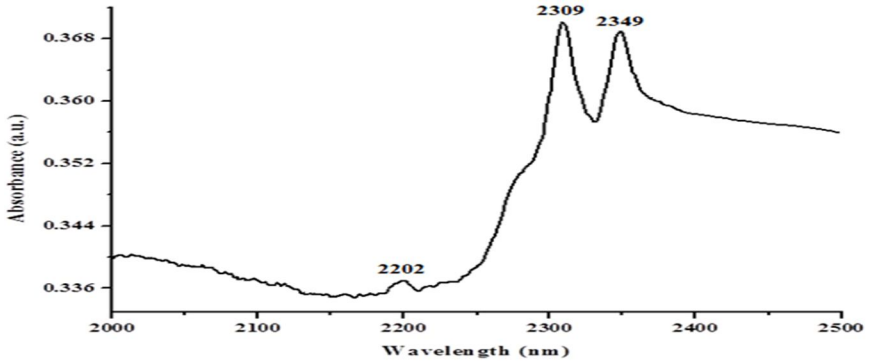

Fig. 5 Optical absorption spectrum of tennantite in the region 2000-2500 nm

4.3 EPR study: The EPR spectrum of tennantite mineral recorded at room temperature (RT) and liquid nitrogen temperature (LNT) as shown in Fig. 6 and Fig. 7 respectively. Tennantite is a copper ore of tetrahedrite group. Though the copper concentration is very high in comparison with iron, the signal due to Cu(II) is not seen because it is hidden under Fe(III) signal for RT spectrum. Cu(II) ions in present mineral is observed from unsymmetrical tetrahedral Fe(III) signal (Fig. 6) and which is also supported by optical absorption spectrum. Fe(III) has five unpaired electrons in weak crystal fields, with a high-spin state ($^6S_{5/2}$). In the X-band EPR spectrum only one signal appears at $g \approx 2.0$ is expected for the perfect T_d or O_h, i.e. cubic ligand fields. The spectrum has single resonance signal at g = 2.357 represents the tetrahedral structure of Fe(III) ions in tennantite mineral at room temperature [20]. In case of LNT EPR spectrum broad and unsymmetrical resolved Cu(II) ion signal is observed with prominent Fe(III) ions. The most intense absorption is attributable to the copper ions and the line becomes rather broad due to the dipolar-dipolar interactions.

As mentioned in the analysis of the optical absorption spectrum, copper ion undergoes elongated tetragonal distortion. Hence, one should expect more than one g-value in the EPR spectrum. The two g- values (parallel, perpendicular) are typical d^9 configuration and possessing axial symmetry with the unpaired electron present in the $d_{x^2-y^2}$ orbital as ground state [21].

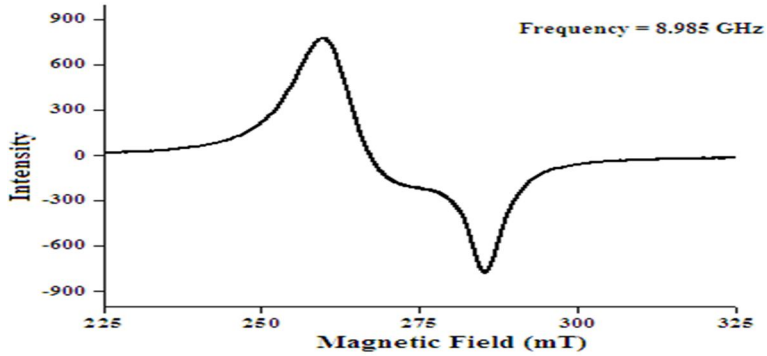

Fig. 6 EPR spectrum of tennantite mineral at RT

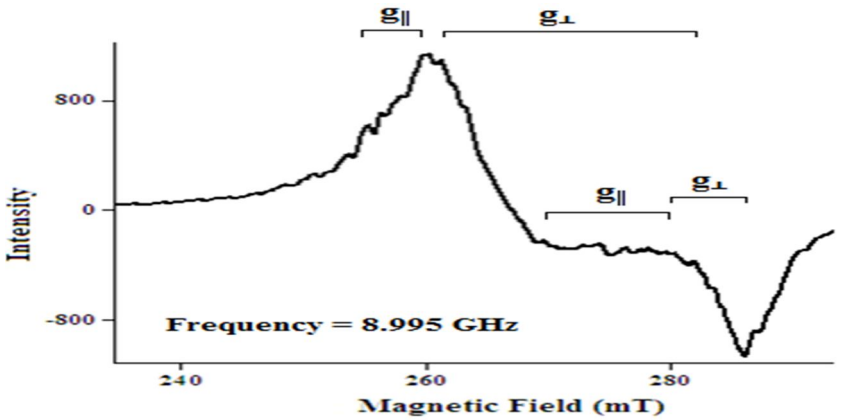

Fig. 7 EPR spectrum of tennantite mineral at LNT

In axial symmetry the g values are related by the expression $G = (g_{\parallel} - g_e)/(g_{\perp} - g_e)$, which measures the exchange interaction between copper centers in the polycrystalline solid. Table 2 gives Spin Hamiltonian and Hyperfine splitting parameters of tennantite mineral at LNT. It is understood that the evaluated spin Hamiltonian (g) and hyperfine splitting (A) parameters suggest Cu(II) ions entered into two different sites, site-I slightly distorted octahedral and site-II in perfectly tetrahedral. The unsymmetrical nature in LNT spectrum also consists of Fe(III) ions in tetrahedral sites. The present g values and G are in tune with other tetrahedral coordinated copper complex [22]. If G > 4, the exchange interaction is negligible; G < 4 indicates considerable exchange interaction. In this mineral, low value of G indicates there is a little strong interaction between Cu ions.

Table 2 Spin Hamiltonian and Hyperfine splitting parameters of tennantite mineral at LNT

Site	$g_{\parallel}$	$g_{\perp}$	$A_{\parallel}$ x 10^{-4} (cm^{-1})	$A_{\perp}$ x 10^{-4} (cm^{-1})	G
I	2.52	2.354	36	95	1.472
II	2.333	2.263	35	42	1.269

4.4 FT-IR Study

FT-IR spectrum of tennantite mineral is shown in Fig. 8. The band at 708 cm^{-1} represents symmetric stretching vibration of As-OH [23]. The band observed at 1030 cm^{-1} can be assigned to S–O stretching vibrations in sulphate [23]. The band observed at 1513 cm^{-1} is attributed to Asymmetric bending of C-O. The peak at 1693 cm^{-1} is assigned to O–H bending. The band at 2359 cm^{-1} is assigned to Atmospheric CO_2 [23]. The fundamental vibrational modes of tennantite mineral are assigned and are presented in Table 3.

Table 3 Vibrational band assignments of tennantite mineral

Vibrational frequency (cm^{-1})	Band assignment
708	Symmetric stretching vibration of As-OH
1030	S–O stretching vibrations in sulphate
1513	Asymmetric bending of C-O
1693	O-H bending
2359	Atmospheric CO_2

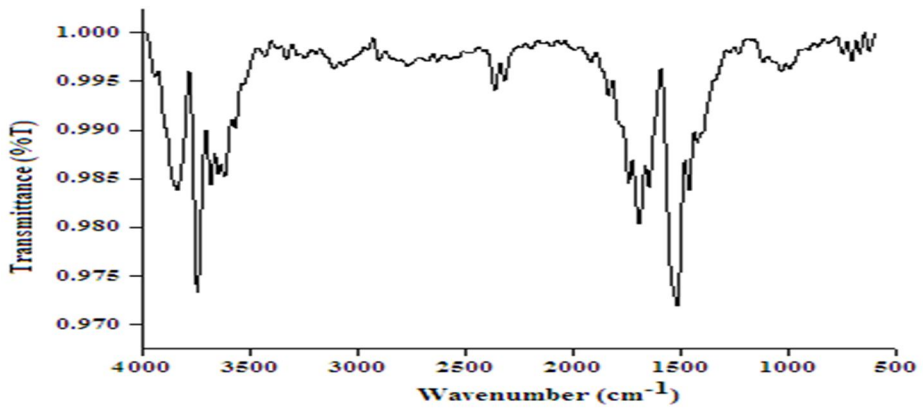

Fig. 8 FT-IR spectrum of tennantite mineral

5 Conclusion

- From powder XRD pattern of tennantite sample, the diffraction data is indexed to a cubic crystal system with JCPDS file no. 43-1478 and the evaluated lattice cell parameter a = 10.2201 Å, which is

almost equal to standard JCPDS data a = 10.2211 Å.

- The average crystallite size is estimated to be 34 nm, which confirms the nanosize. The average strain and dislocation density of collected sample was calculated as ε_{str} = 0.283 x 10^{-3} and δ = 0.122 x 10^{15} lines/m.
- Optical absorption spectrum exhibited characteristic bands of Fe(III) and Cu(II) in tetrahedral site symmetry. In the case of Cu(II) ions it is further distortion tetragonally distorted octahedral. The crystal field and Racah parameters are evaluated for Fe(III) ions. Crystal field and tetragonal field parameters for Cu(II) ions are also evaluated.
- EPR spectra of RT & LNT shows the presence of both Fe(III) and Cu(II) ions in the mineral. In case of Cu(II) ions, it occupies different sites which supports LNT spectrum. Similarly, octahedral coordinated Cu(II) ions also observed. The evaluated g and A values are in tune with other Cu(II) bearing minerals.
- FT-IR spectrum of tennantite mineral exhibited various characteristic vibrational bands of As-OH, S-O, C-O and hydroxyl ions.

6 Acknowledgements: The authors wish to express their thanks Mr. F. Ebbult, Institute of Mineralogy and Petrograph, ETH Zentrum, Switzerland for donating the mineral sample.

7 References

[1] S.V.J. Lakshman, B.J. Reddy, Can. Min. 12 (1973) 207.
[2] F. Habashi, Metals from ores: an introduction to extractive metallurgy, Metallurgie Extractive Quebec, Sainte Foy, Quebec (2003).
[3] R.R. Moskalyk, A.M. Alfantazi, Review of copper pyrometallurgical practice: today and tomorrow, Min. Engg. 16 (2003) 893.
[4] W.G. Davenport, M. King, M. Schlesinger, A.K. Biswas, Extractive Metallurgy of copper, 4th Eds., Elsevier Science Ltd., Oxford, UK (2002).
[5] T. Wagner, E. Jonsson, Can. Min. 39 (2001) 855.
[6] R.L. Allen, P. Weihed, S. Svenson, Eco. Geo. 91 (1996) 1022.
[7] L. Curreli, C. Garbarino, M. Ghiani, G. Orru, Hydrometallurgy 96 (2009) 258.
[8] P. Lattanzi, S. Da Pelo, E. Musu, D. Atzei, B. Elsener, M. Fantauzzi, A. Rossi, Ear. Sci. Rev. 86 (2008) 62.
[9] D. Filippou, P. St-Germain, T. Grammatikopoulos, Min. Proc. Extra. Metallu. Rev. 28 (2007) 247.
[10] S. Vedanand, B. Madhusudhan, B.J. Reddy, P.S. Rao, Bull. Mat. Sci. 19 (1996) 1089.
[11] W. Tongamp, Y. Takasaki, A. Shibayama, Hydrometallurgy 98 (2009) 213.
[12] S.V.J. Lakshman, B.J. Reddy, K. Janardhanam, V.L.R. Murthy, P. Rama Devi, Czech. J. Phys. B. 28 (1978) 1122.
[13] B.J. Reddy, K.B.N. Sharma, Solid State Commu. 38 (1981) 547.
[14] B.J. Reddy, J. Yamauchi, M. Venkata Ramanaiah, A.V.

Chandrasekhar, R.V.S.S.N. Ravikumar, Rad. Eff. Def. Solids 159 (2004) 141.
[15] M. Venkata Ramanaiah, R.V.S.S.N. Ravikumar, A.V. Chandrasekhar, B.J. Reddy, Y.P. Reddy, P.S. Rao, Ferroelectrics 216 (1998) 27.
[16] R. Rama Subba Reddy, Md. Fayazuddin, G. Siva Reddy, S. Lakshmi Reddy, P. Sambasiva Rao, B.J. Reddy, F. Nieto Grcia, Cryst. Res. Technol. 39 (2004) 240.
[17] K.R. Murali, A. Kalaivanan, S. Perumal, N. Neelakanda Pillai, J. Alloys Compd. 503 (2010) 350.
[18] S. Venkatachalam, R.T. Rajendrakumar, D. Mangalaraj, S. Narayandass, K. Kim, J. Yi, Solid State Electron. 48 (2004) 2219.
[19] M. Venkata Ramanaiah, R.V.S.S.N. Ravikumar, A.V. Chandrasekhar, B.J. Reddy, Y.P. Reddy, P.S. Rao, Ferroelectrics 216 (1998) 27.
[20] S. Lakshmi Reddy, Md. Fayazuddin, N.C. Gangi Reddy, Tamio Endo, R.L. Frost, Rad. Eff. Def. Solids 163(2008) 19.
[21] B.J. Hathaway, J. Chem. Soc., Dalton Trans., 1196 (1972).
[22] F. Jian, P. Zhao, H. Wang, L. Lu, Bull. Korean Chem. Soc. 25 (2004) 673.
[23] Y. Brechbuhl, I. Christl, E.J. Elzinga, R. Kretzschmar, J. Colloid Inter. Sci. 377 (2012) 313.